Simulation of dilute solutions of linear and star-branched polymers by dissipative particle dynamics

M. M. Nardai and G. Zifferer[a)]
Department of Physical Chemistry, University of Vienna, Währinger Str. 42, A-1090 Wien, Austria

(Received 24 July 2009; accepted 28 August 2009; published online 24 September 2009)

A most promising off-lattice technique in order to simulate not only static but in addition dynamic behavior of linear and star-branched chains is the dissipative particle dynamics (DPD) method. In this model the atomistic representation of polymer molecules is replaced by a (coarse-grained) equivalent chain consisting of beads which are repulsive for each other in order to mimic the excluded volume effect (successive beads in addition are linked by springs). Likewise solvent molecules are combined to beads which in turn are repulsive for each other as well as for the polymer segments. The system is relaxed by molecular dynamics solving Newton's laws under the influence of short ranged conservative forces (i.e., repulsion between nonbonded beads and a proper balance of repulsion and attraction between bonded segments) and dissipative forces due to friction between particles, the latter representing the thermostat in conjunction with proper random forces. A variation of the strength of the repulsion between different types of beads allows the simulation of any desired thermodynamic situation. Static and dynamic properties of isolated linear and star-branched chains embedded in athermal, exothermal, and endothermal solvent are presented and theta conditions are examined. The generally accepted scaling concept for athermal systems is fairly well reproduced by linear and star-branched DPD chains and theta conditions appear for a unique parameter independent of functionality as in the case of Monte Carlo simulations. Furthermore, the correspondence between DPD and Monte Carlo data referring to the shape of chains and stars is fairly well, too. For dilute solutions the Zimm behavior is expected for dynamic properties which is indeed realized in DPD systems. © *2009 American Institute of Physics*. [doi:10.1063/1.3231854]

I. INTRODUCTION

In general, characteristic properties of polymer molecules fluctuate around mean values due to continuous changes in shape and size, which may be a examined by use of simulation methods,[1–5] i.e., by molecular dynamics (MD) or Monte Carlo (MC) calculations, in a highly efficient manner. Depending on the method chosen, atomistic details are more or less perfectly considered or almost ignored.[6] Approximations are minimal in quantum mechanical calculations from first principles. These methods become enormously exhaustive for a larger number of atoms and thus are restricted to rather small systems only. Larger systems of size $(5–10\ \mathrm{nm})^3$ over a time interval of several nanoseconds may be simulated by use of atomistic molecular dynamics (AMD) based on proper force fields.[7] However, for polymer systems, length scales of structural properties (size of a bond $\ll$ size of coils) as well as time scales of dynamic properties are spread over several orders of magnitude.[1] Therefore, further simplifications of the models are necessary. One route is to replace groups of atoms (for example, CH_3–, CH_2–, etc., or still larger units such as a monomer) by a single unit (united atoms model) and another is to combine groups of monomers to single segments (coarse-grained chains). The former treatment allows for quasiatomistic simulations[8] by applying proper potentials (between units instead of atoms as in the case of AMD). The latter typically leads to mesoscale simulations applying more simple potentials characterizing the principal behavior of interactions between chain segments only.[9] This procedure makes sense because chain molecules have a very large number of internal degrees of freedom. Thus, a practically infinite number of possible configurations make the details of interaction of minor importance for general properties. Furthermore, the chain length (here the number of segments of the model chain) still serves as an independent parameter which allows the calculation of a wide range of universal features depending on this parameter.

As long as static properties of linear chains are of interest only, lattice based MC techniques are preferred which explore the phase space in an extremely efficient stochastic way, thus yielding ensemble averages from a (large) number of randomly taken snapshots of the system. In case of star-branched polymers the segment density near the center of the star is larger the larger the number of arms is; in the tetrahedral lattice, e.g., up to 12 arms may be connected to a central core consisting of a central lattice point and its four neighbors;[10] the innermost $1+4+12=17$ segments, however, are fixed in space and cannot be relaxed by the usual methods.[11] Thus, simulations of star-branched chains based on simple lattice models only make sense in the high dilution limit where either properties of single molecules are calcu-

[a)]Author to whom correspondence should be addressed. Electronic mail: gerhard.zifferer@univie.ac.at.

lated (infinite dilution) or the limiting (linear) concentration dependence of characteristic properties are evaluated from pairs of molecules placed in all possible relative distances (and orientations).

For multichain simulations, however, movement of the core is absolutely necessary. This may be a reason that properties of single stars are relatively well investigated, e.g., see Refs. 12–22 and the impressively long list of references in Freire's review[23] and in our feature article,[11] while the concentration dependence of properties of branched (homo)polymers is less explored.[24–33]

However, mobility of the center is also necessary for single star-branched chains if dynamic properties such as diffusion coefficients are of interest in addition to static properties such as size and shape of the molecules. In order to mobilize the core of the star the so-called bond fluctuation model[33–35] (or some other high coordination lattice[25]) may be used. An appropriate method for the simulation of polymer melts (including branched polymers) is the cooperative motion algorithm of Pakula *et al.*[26] Another route for the simulation of melts is studies with soft potentials which allow for double occupancies of lattice positions.[36,37] For the simulation of the dynamics of polymers in solution multiparticle-collision dynamics[38] may be combined[39] with MD, a method which also has been used for the simulation of star-branched chains.[40] The dissipative particle dynamics (DPD) simulation technique[41]—being capable of giving semiquantitative predictions for specific monomer/solvent interactions[42]—is most promising for any type of mesoscale simulations but scarcely[43–47] applied so far to star-branched polymers. By use of this latter method (which is suitable for the total range of concentrations from a single solute molecule up to a solvent free melt), in the present paper static as well as dynamic properties of highly diluted star-branched polymers are investigated: First, scaling laws of global properties in athermal (good) solvent are discussed in dependence on chain length and degree of branching. Second, pseudoideal (theta) conditions are determined for the DPD model. Third, so called g-factors for athermal and theta conditions are given and compared to theoretical predictions. Fourth, quantities characteristic of the instantaneous shape of linear chains and stars are discussed as functions of the thermodynamic quality of the solvent and compared to MC results. Last, the diffusion coefficient of DPD coils is studied in some detail.

II. COMPUTATIONAL METHOD

DPD (Refs. 41 and 42) smoothly covers the range from several nanometers up to the mesoscale region. In this model the atomistic representation of the polymer molecules is replaced by a (coarse-grained) equivalent chain. Monomers as well as solvent molecules are combined to beads which are repulsive for each other in order to mimic the excluded volume effect. In addition, successive beads within polymer molecules are linked together by use of springs. Thus, polymer chains evolve in a bath of single beads, which act as the solvent. The explicit treatment of the solvent and the preservation of Galilean invariance due to a proper combination of random and friction forces in strictly pairwise interaction (see below) give rise to momentum transport within the fluid and thus allow for correct hydrodynamic interaction.[48] Furthermore, a variation of the strength of the repulsion between different types of beads allows the simulation of any desired thermodynamic situation.

The algorithm adopted closely follows the original one, see Ref. 42, i.e., the system is relaxed by MD solving Newton's laws in dimensionless representation,

$$\frac{d\mathbf{r}_i}{dt} = \mathbf{v}_i, \quad \frac{d\mathbf{v}_i}{dt} = \mathbf{f}_i = \sum_{j \neq i} (\mathbf{f}_{ij}^c + \mathbf{f}_{ij}^d + \mathbf{f}_{ij}^r), \tag{1}$$

$$(\mathbf{f}_{ji} = -\mathbf{f}_{ij}), \quad \mathbf{f}_i = (f_{i,x}, f_{i,y}, f_{i,z}),$$

based on reduced time

$$t = t^{\text{real}}/t_c, \quad t_c = \sqrt{Mr_c^2/k_BT}, \tag{2}$$

assuming equal mass M for all beads with position

$$\mathbf{r}_i = \mathbf{r}_i^{\text{real}}/r_c \tag{3}$$

(in multiples of the cutoff radius r_c) and reduced velocity

$$\mathbf{v}_i = \mathbf{v}_i^{\text{real}}/\sqrt{k_BT/M} \tag{4}$$

under the influence of the (accordingly reduced) force

$$\mathbf{f}_i = \mathbf{f}_i^{\text{real}}/(k_BT/r_c) \tag{5}$$

consisting of (short ranged) *conservative forces*, i.e., repulsion between nonbonded beads and a proper balance of repulsion and attraction between bonded segments,

$$\mathbf{f}_{ij}^c = \begin{cases} a_{ij}(1-r_{ij})\mathbf{r}_{ij}/r_{ij} - b_{ij}\mathbf{r}_{ij}, & r_{ij} < 1, \\ -b_{ij}\mathbf{r}_{ij}, & r_{ij} \geq 1, \end{cases}$$

$$b_{ij} = \begin{cases} b & i \text{ connected to } j \\ 0 & \text{otherwise} \end{cases} \tag{6}$$

using the abbreviation

$$\mathbf{r}_{ij} = \mathbf{r}_i - \mathbf{r}_j, \quad r_{ij} = |\mathbf{r}_{ij}|, \tag{7}$$

dissipative forces (due to friction between particles)

$$\mathbf{f}_{ij}^d = \begin{cases} -\gamma(1-r_{ij})^2((\mathbf{v}_i - \mathbf{v}_j)\mathbf{r}_{ij}/r_{ij})\mathbf{r}_{ij}/r_{ij}, & r_{ij} < 1, \\ 0, & r_{ij} \geq 1, \end{cases} \tag{8}$$

and *random forces* (representing the thermostat together with the latter one)

$$\mathbf{f}_{ij}^r = \begin{cases} \sqrt{2\gamma/\Delta t}(1-r_{ij})\xi_{ij}\mathbf{r}_{ij}/r_{ij}, & r_{ij} < 1, \\ 0, & r_{ij} \geq 1, \end{cases} \tag{9}$$

with ξ_{ij} the Gaussian distributed random number and Δt the (reduced) time step. The simulation is performed by use of a slightly modified Verlet velocity algorithm within a simulation box with periodic boundaries in all directions.

As already stated, parameters a_{ij} (giving the strength of repulsion in units of k_BT with k_B being Boltzmann's constant and T representing absolute temperature) are dependent on the type of beads i and j, respectively, and read as a_{PP} if both beads belong to a polymer chain, $a_{\text{PS}}=a_{\text{SP}}$ if one bead is a polymer segment and the other a solvent, and a_{SS} for the interaction between two solvent beads. Simulation param-

eters have been chosen according to Ref. 42, i.e., $\Delta t=0.04$, $\gamma=4.5$, total particle density $\rho=3$, $a_{PP}=a_{SS}=25$, and $b=4$. While $a_{PP}=a_{SS}$ are fixed, $a_{PS}=a_{SP}$ are varied in order to mimic different solvent conditions, the case $a_{PS}=a_{PP}$ referring to athermal conditions, $a_{PS}<a_{PP}$ being characteristic for an exothermal solution, and $a_{PS}>a_{PP}$ for an endothermal one.

Depending on the average size of the solute, the edge lengths of the simulation box was chosen in the range from 10 to 90 (approximately five times the average radius of the solute in order to avoid interaction of periodic images[49,50]) for star-branched chains having $F=2$ (linear) to $F=12$ arms, with $m=2$ to $m=256$ beads per arm, yielding a total number of segments $N=mF+1$ up to a rather large value $N=3073$. Results are based on 400 000 to 800 000 samples applying five time steps between two sampled systems corresponding to a total simulation time of $(80-160)\times 10^3 t_c$. Error bars are obtained by the block averaging method[51] and are omitted in the diagrams if smaller than the symbol size as well as in case of extrapolated data.

III. RESULTS AND DISCUSSION

A. Athermal systems

For ideal chains and stars (unperturbed random walks) mean square dimensions $\langle x^2\rangle$ increase proportionally to the total number of bonds $n=N-1$. Examples for x^2, calculated in the present paper, are the squared radius of gyration, s^2, i.e., the mean of squared distances of beads from their common center of gravity, the squared end-to-end distance, h^2, and the squared center-to-end distance, r^2, the latter two actually being averages of $F(F-1)/2$ and F, respectively, squared distances.

For nonideal systems, $\langle x^2\rangle$ should exhibit a scaling behavior $\langle x^2\rangle \sim n^{2\nu}$ again with ideal scaling $2\nu=1$ in case of pseudoideal (theta) conditions. Above theta conditions an exponent characteristic of good solvent conditions, $2\nu=1.176$, should be found while below theta conditions a collapse into a condensed state should occur yielding an exponent $2\nu=2/3$. In the limit of infinitely long polymers a sharp transition between states should occur at the theta point. However, for finite chain length a smooth variation of the exponent 2ν on solvent condition is expected. For athermal conditions MC simulations of rather large linear and star-branched athermal chains confirm not only $2\nu=1.176$ but also the type of short-chain correction as provided by renormalization group theory,[52]

$$\langle x^2\rangle = A_x n^{2\nu}(1 + B_x n^{-\Delta} + \cdots), \tag{10}$$

with $\Delta=0.478\approx 1/2$. For (rather short) linear DPD chains exponents ranging from 1.04 to 1.16 are reported for athermal conditions.[53–58] This nearly "ideal" scaling in some cases was attributed to a certain violation of the excluded volume condition due to possibly unphysical crossing of bonds (springs) during relaxation. Studies of the behavior of catenalike ring shaped DPD chains gave some evidence that such forbidden crossings actually occur.[56] In Fig. 1 log-log plots of $\langle s^2\rangle$, $\langle h^2\rangle$, and $\langle r^2\rangle$ versus n are shown. For larger chain lengths the data are fairly well located on straight lines

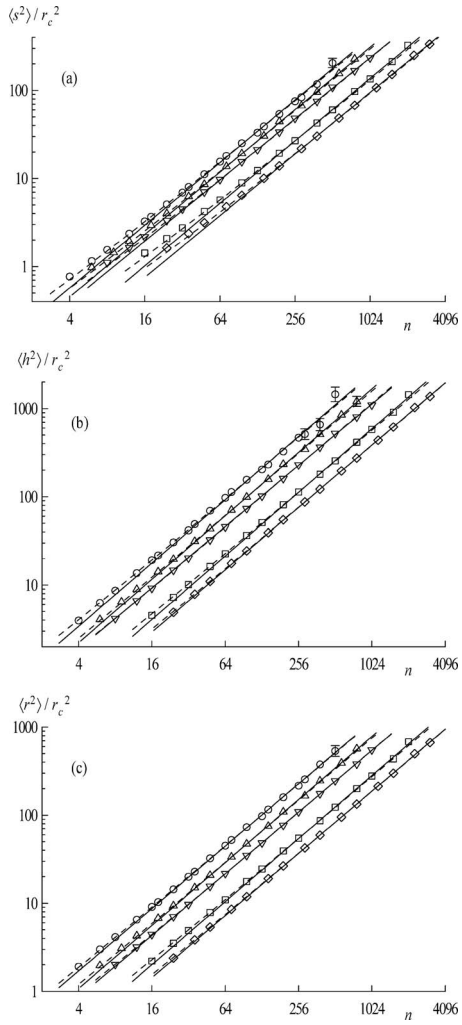

FIG. 1. Log-log plots of (a) mean square radius of gyration, (b) mean square end-to-end distance, and (c) mean square center-to-end distance vs total number of bonds n of linear chains (circles) and stars with $F=3$ (triangles), $F=4$ (inverted triangles), $F=8$ (squares) and $F=12$ (diamonds) arms. Athermal conditions ($a_{PS}=25$). Straight lines result from linear regression ($m\geq 24$ and $n\geq 64$); slopes for $F=2-12$ read as (a) 1.181, 1.177, 1.153, 1.178, and 1.162, (b) 1.191, 1.194, 1.153, 1.196, and 1.173, and (c) 1.177, 1.188, 1.163, 1.189, and 1.172. Broken lines calculated by Eq. (10) using data given in Table I.

while for smaller chain lengths curvature toward larger values appears. Restricting linear regression to $m\geq 24$ and $n\geq 64$, i.e., a minimum arm length of 24 for stars and 32 for $F=2$ results in slopes between 1.15 and 1.18. However, fitting $\langle x^2\rangle/n^{1.176}$ versus $n^{-1/2}$ to straight lines yields parameters A_x and B_x of Eq. (10) (given in Table I) which fairly well

TABLE I. Coefficients A_x and B_x of short-chain correction according to Eq. (10) for mean square dimensions of athermal star-branched chains with F arms.

F	A_s	B_s	A_h	B_h	A_r	B_r
2	0.1082	0.586	0.6850	0.311	0.3278	0.237
3	0.0833	0.672	0.4524	0.159	0.2148	0.189
4	0.0651	0.969	0.3276	0.310	0.1555	0.366
8	0.0361	1.503	0.1612	0.496	0.0778	0.506
12	0.0254	1.781	0.1089	0.473	0.0529	0.476

represent the data as shown in Fig. 1 (broken line). Admittedly, scattering of $\langle x^2\rangle/n^{1.176}$ is rather large and a fit versus $1/n$ would be possible too, as occasionally suggested for linear DPD chains.[57,59] Nevertheless it may be concluded from our results that the generally accepted scaling concept for athermal systems is fairly well reproduced by linear and star-branched DPD chains.

B. Theta systems

As mentioned above ideal and pseudoideal, respectively, conditions are characterized by a scaling behavior $\langle x^2\rangle \sim n^{2\nu}$ with $2\nu=1$. In an experimental environment pseudoideal behavior occurs in special endothermal solvents (theta solvents) at a certain temperature (theta or Flory temperature). Likewise in computer simulations the quality of the implicit or explicit solvent is controlled by energy parameters. In DPD the (repulsive) interaction parameter a_{PS} between polymer segments and solvent beads may be varied while for segment-segment and solvent-solvent interactions the parameters $a_{SS}=a_{PP}$ are fixed at the initial value reading as 25 in the present study. Based on rather short linear chains Schlijper *et al.*[53] as well as Kong *et al.*,[54] the latter applying a_{PS} values in the range 17.5–32.5, expected theta behavior near athermal conditions; a reliable theta value, however, is not available so far to our best knowledge. Thus, we calculated the chain length dependence of $\langle s^2\rangle$, $\langle h^2\rangle$, and $\langle r^2\rangle$ of linear and star-branched chains in the a_{PS} range suggested by Kong *et al.* in order to obtain the DPD theta parameter. First, we extracted the theta parameter directly from the dependence of 2ν on a_{PS} (taking 2ν from the slopes of linear regressions of data points $\log\langle x^2\rangle$ versus $\log n$) shown in Fig. 2. For $a_{PS}<25$ (exothermal conditions) exponents slightly increase with decreasing a_{PS} while for $a_{PS}>25$ (endothermal conditions) the exponents rapidly decrease, take a value of 1 at $a_{PS}\approx 27.2$ for all functionalities and squared distances evaluated, and then further decrease until $a_{PS}=30$ reaching values roughly corresponding to collapsed chains (characterized by $2\nu=2/3$). Although not relevant for the determination of the theta parameter it should be mentioned that log-log plots of mean square dimensions versus chain lengths for $a_{PS}\geq 30$ show a slight curvature (the slope increasing with increasing chain length) which is more pronounced the smaller the number of arms is. Obviously, chain collapse is easier for longer linear chains than for shorter ones for geometrical reasons while already symmetric 12-arm stars are compressed into more or less perfect coils at even comparably short lengths. Thus, based on an average slope in the range of chain lengths evaluated (the maximum chain length increasing with increasing number of arms), for $F=12$ the exponent (≈ 0.6) is already near the expected value of 2/3 while still smaller values are found for stars with a fewer number of arms and for linear chains.

In Table II theta parameters for $F=2$ to 12 for $\langle s^2\rangle$, $\langle h^2\rangle$, and $\langle r^2\rangle$ are given, obtained from the intersection of the linear interpolation curves and the (broken) horizontal line with the intercept one, shown in Fig. 2, together with interpolated values of prefactors (proportionality constants between $\langle x^2\rangle$ and n). These results are corroborated by a second analysis

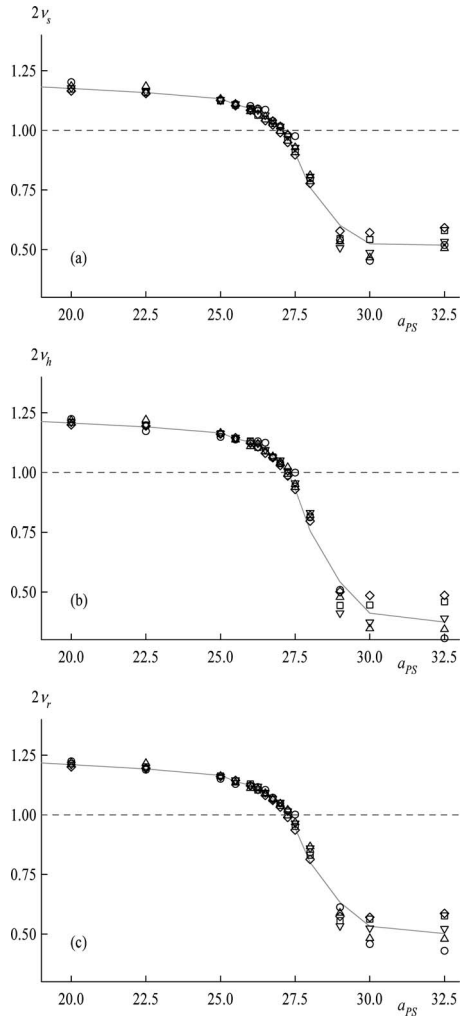

FIG. 2. Scaling exponents for (a) mean square radius of gyration, (b) mean square end-to-end distance, and (c) mean square center-to-end distance as functions of the polymer-solvent parameter a_{PS}. Symbols as in Fig. 1; the gray line is a guide to the eye only.

based on the fact that ratios $\langle x^2\rangle/n$ or $\langle x^2\rangle/m$ should be independent of n and m, respectively, for theta conditions (ignoring logarithmic correction terms postulated for theta conditions). Thus, $\langle x^2\rangle/n$ as functions of a_{PS} for constant values of n should intersect in a single point characterizing the theta parameter. The method is demonstrated in Fig. 3 for an arbitrary system ($F=8$, $\langle r^2\rangle$) and all results are summarized in Table III. The values actually are averages of all possible crossing points, abscissas referring to $a_{PS,\theta}$ and ordinates are estimates of prefactors $A_{x,\theta}$ of scaling laws $\langle x^2\rangle=A_{x,\theta}n$.

TABLE II. Theta parameters for star-branched chains with F arms obtained by the procedures depicted in Fig. 2 and accordingly obtained prefactors of scaling laws $\langle x^2\rangle=A_{x,\theta}n$ of mean square dimensions.

F	$a_{PS,\theta}$	$A_{s,\theta}$	$a_{PS,\theta}$	$A_{h,\theta}$	$a_{PS,\theta}$	$A_{r,\theta}$
2	27.12	0.1649	27.19	0.9373	27.50	0.4411
3	27.12	0.1334	27.33	0.6208	27.35	0.3077
4	27.10	0.1120	27.28	0.4842	27.33	0.2386
8	27.00	0.0710	27.23	0.2665	27.25	0.1309
12	26.93	0.0541	27.17	0.1937	27.19	0.0951

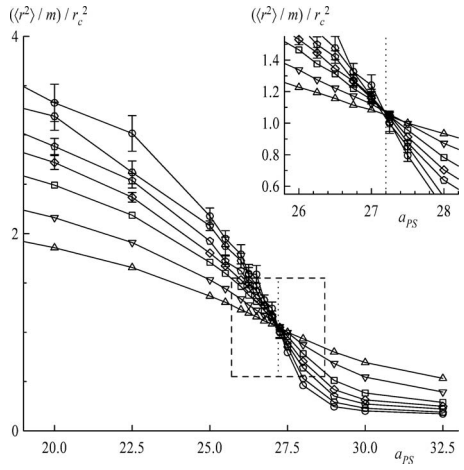

FIG. 3. Ratios of the mean square center-to-end distances and arm length m of star-branched chains with $F=8$ arms as a function of the polymer-solvent parameter a_{PS} for constant values of m, i.e., $m=8$ (triangles) to $m=128$ (circles).

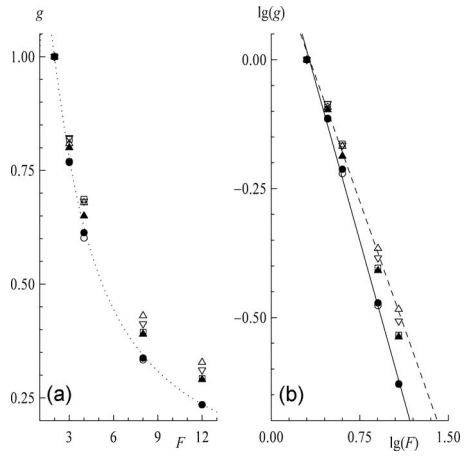

FIG. 4. g-values vs number of arms F for athermal and theta conditions obtained by DPD (open symbols) compared to results of MC simulations (Ref. 11) (full symbols) in a (a) conventional plot and (b) log-log plot. Circles (triangles) refer to athermal (theta) conditions calculated from prefactors of scaling laws; the dotted line in (a) is calculated by use of Eq. (13); the straight lines in (b) with slopes −0.82 (full line) and −0.64 (broken line) result from linear regression. Results for $a_{PS}=27.25$ (near theta conditions) are given in addition (squares).

The $a_{PS,\theta}$ values range from 27.00 to 27.30 and slightly increase from $\langle s^2\rangle$ over $\langle h^2\rangle$ to $\langle r^2\rangle$; however, as already stated above, no systematic dependence of a_{PS} on F is found in full accordance with MC models which—based on implicit solvent—also result in a unique theta value for linear chains and stars.[11]

C. Size of DPD stars and chains

A quantity common in use to compare the size of star-branched polymers with the size of linear chains is the ratio of mean square radii of gyration of stars and linear chains with equal number of segments, $g=\langle s^2\rangle_F/\langle s^2\rangle_{F=2}$. According to scaling arguments of Daoud and Cotton[60] and Birshtein and Zhulina,[61] star-shaped polymers may be divided into three parts, (a) a central core of constant density, (b) an intermediate part exhibiting bulk behavior, and (c) an outside shell where the branches are more or less independent, thus exhibiting behavior of isolated chains. The model [strictly speaking part (c) of the model] results in the scaling law

$$\langle s^2\rangle \sim m^{2\nu}F^{1-\nu} = n^{2\nu}F^{1-3\nu}, \tag{11}$$

and thus

$$g \sim F^{1-3\nu}. \tag{12}$$

For athermal systems, Eq. (12) is in good accordance with experimental and simulation data.[11,24,62] Interestingly, at least for a small number of arms, g-values of athermal stars[11,23,24] also fairly well coincide with

$$g \sim \frac{3F-2}{F^2}, \tag{13}$$

developed by Zimm and Stockmayer for random walk stars.[63] As pseudoideal behavior results from compensation, for theta systems coils are expanded as compared to random walks, the expansion increasing with increasing functionality.[11,61,64] Thus, g-values of theta stars are larger than those of random walk stars [Eq. (13)] and scale like $F^{-0.7}$, see Refs. 11, 24, 65, and 66, instead of $F^{-0.5}$ as predicted by Eq. (12). In Fig. 4 g-values of DPD stars (calculated from the prefactors of scaling laws, A_s and $A_{s,\theta}$, respectively) are depicted together with MC results in a conventional plot [Fig. 4(a)] and a log-log plot [Fig. 4(b)]. In Fig. 4(a) the prediction for random walks [Eq. (13)] is shown for comparison. The correspondence between DPD and MC data is fairly well for athermal and reasonable for theta conditions. In addition, g-values for a system near theta conditions ($a_{PS}=27.25$) are shown to be in good agreement with MC results. Scaling exponents extracted from Fig. 4(b) read as −0.82 (athermal DPD stars) and −0.64 (theta DPD stars), the former value roughly in correspondence with theory ($-0.764\approx-0.8$) and the latter one again slightly more negative than −0.50, in accordance with MC results. For rather large values of $a_{PS}\geq 30.0$, $g\approx 1$ throughout, again demonstrating collapse in this region of parameters[67] (not shown).

TABLE III. Theta parameters for star-branched chains with F arms obtained by the procedures depicted in Fig. 3 and accordingly obtained prefactors of scaling laws $\langle x^2\rangle=A_{x,\theta}n$ of mean square dimensions.

F	$a_{PS,\theta}$	$A_{s,\theta}$	$a_{PS,\theta}$	$A_{h,\theta}$	$a_{PS,\theta}$	$A_{r,\theta}$
2	27.15	0.1646	27.17	0.9583	27.14	0.4890
3	27.10	0.1353	27.10	0.6798	27.14	0.3274
4	27.12	0.1123	27.16	0.5096	27.17	0.2528
8	27.10	0.0679	27.15	0.2752	27.15	0.1362
12	27.08	0.0512	27.14	0.1955	27.14	0.0965

D. Shape of DPD stars and chains

Based on the concept of "equivalent ellipsoids" introduced by Šolc and Stockmayer[68,69] by calculating the orthogonal components L_i^2 (which by definition are chosen as $L_1^2\leq L_2^2\leq L_3^2$) of the squared radius of gyration $s^2=L_1^2+L_2^2+L_3^2$ taken along the principal axes of inertia, several quantities characteristic of the instantaneous shape of the coil may

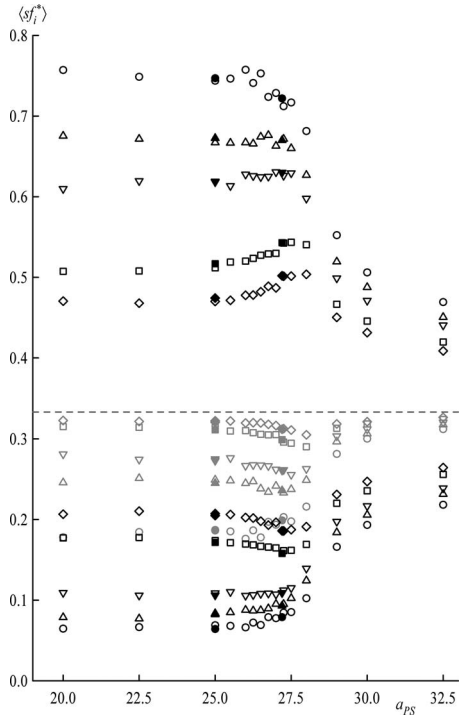

FIG. 5. Shape factors vs polymer-solvent parameter a_{PS}. The value of 1/3 expected for perfectly symmetric coils is indicated by the broken line. MC results are given for comparison (Ref. 11) (full symbols). Types of symbols are as in Fig. 1.

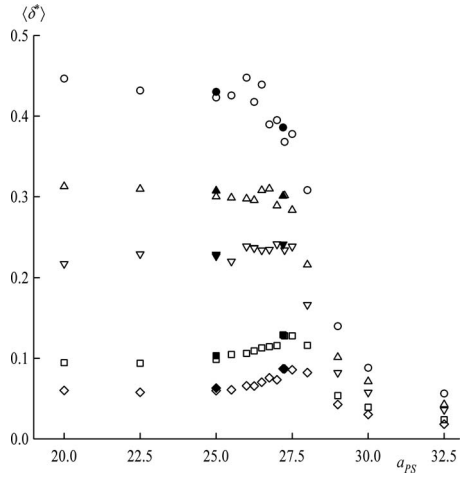

FIG. 6. Asphericity parameter vs polymer-solvent parameter a_{PS}. MC results are given for comparison (Ref. 11) (full symbols). Types of symbols are as in Fig. 1.

be deduced.[70] In order to compare configurations of different sizes it is advantageous to use reduced components (shape factors),

$$sf_i^* = L_i^2/s^2, \tag{14}$$

which in turn define an asphericity parameter,

$$\delta^* = 1 - 3(sf_1^* sf_2^* + sf_2^* sf_3^* + sf_3^* sf_1^*), \tag{15}$$

ranging from 0 (perfect symmetry, i.e., a sphere) to 1 (rodlike chain). In Fig. 5 shape factors (extrapolated to $n \to \infty$) are given as functions of parameters a_{PS}. For comparison MC results for athermal and theta systems are given in addition. An analogous diagram for the asphericity parameter is shown in Fig. 6. In accordance with MC data athermal stars are slightly more symmetric than theta stars, as the arms of the star have to avoid each other due to the excluded volume, an effect which is slightly diminished in endothermal environment due to less repulsive interaction between polymer segments as compared to solvent beads. For large values of a_{PS} shape factors approach the value of 1/3 (characteristic of a sphere) again compatible with chain collapse, although only the intermediate shape factor actually reaches the limiting value 1/3, and δ^* is still slightly larger than zero.

E. Mobility of DPD stars and chains

The discussion above clearly shows that the behavior of DPD chains and stars is in full accordance with other simulation results, at least concerning static properties. However, the major drawback of MC simulations (at least for highly diluted systems) is that (at best) the Rouse behavior[71] may be expected for MC dynamics simulations for lack of hydrodynamic interaction between the solvent and solute.[1] The Rouse behavior is reasonable in more concentrated solutions and bulk (at least for short chains) but definitely in contradiction to experimental results in the limit of high dilution where the diffusion coefficient scales according to Zimm.[72]

Contrary to MC approaches, in DPD the solvent is explicitly available and the interplay of random forces and friction results in a correct treatment of hydrodynamic interaction. Furthermore, the time scale is large enough to allow a direct calculation of the diffusion coefficient D from the time evolution of mean square displacements, thus avoiding the use of further approximations, e.g., correspondence between diffusion coefficient and hydrodynamic radius provided by Kirkwood and Riseman.[73]

D may be extracted from the limiting slope from a plot of the mean square displacement (msd) of the center of gravity of the molecules versus time,

$$D = \frac{1}{6} \lim_{t \to \infty} \frac{d\text{msd}}{dt}, \tag{16}$$

where

$$\text{msd} = \langle |\mathbf{r}_{\text{cog}}(t) - \mathbf{r}_{\text{cog}}(0)|^2 \rangle \tag{17}$$

and $\boldsymbol{r}_{\text{cog}}(t)$ is the position of the center of gravity at a particular time.[74]

In Fig. 7 log-log plots of the diffusion coefficient versus n of a single 12-arm star in athermal solvent, theta solvent, and in a solvent of still worse quality are shown. Data points are located on straight lines with slopes (calculated by linear regression) reading as -0.61 (athermal system), -0.48 (theta system), and -0.31 (collapsed region). Thus, actually the power law $D \sim n^{-\nu}$ is fairly well satisfied, with exponents being approximately equal to the expected values (-0.588, -0.5, and $-1/3$). It should be noted that simulations on linear chains[49,58] revealed a certain dependence of D on the size of the box. Dünweg and Kremer suggested a correction function proportional to the box length in multiples of the radius of gyration.[75] In the present case such a correction function actually degenerates into a constant as the box lengths have

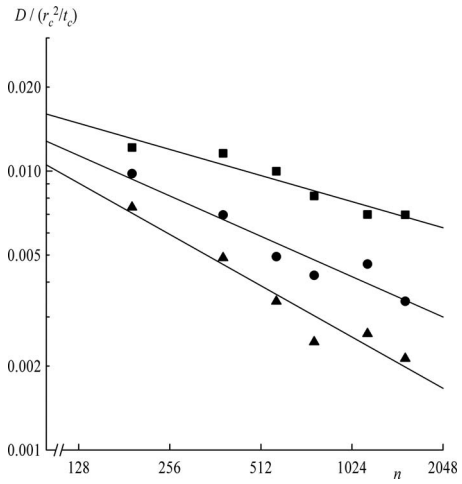

FIG. 7. Diffusion coefficients obtained from mean squared displacements of star-branched chains with $F=12$ arms for $a_{PS}=25$ (triangles), $a_{PS}=27.25$ (circles), and $a_{PS}=30.0$ (squares). Straight lines with slopes -0.61, -0.48, and -0.31 result from linear regression.

been chosen to be $\approx 5\langle s^2\rangle^{1/2}$ as stated in Sec. II. Admittedly, the value of the constant is unknown, but it leaves the exponent unchanged.

In Fig. 8 log-log plots of the translational diffusion time $\tau_D=\langle s^2\rangle/D$ (characterizing the time necessary in order to reach a squared distance comparable to the size of the coil) versus n are shown for athermal and theta systems at constant F. Starting with Eq. (11) for $\langle s^2\rangle$ and the predictions $D\sim n^{-1}$ (Rouse) and $D\sim\langle s^2\rangle^{-1/2}$ (Zimm), respectively, the following scaling laws should be valid:[23,24]

$$\tau_D \sim \begin{cases} n^{2\nu+1}F^{1-3\nu} = m^{2\nu+1}F^{2-v}, & \text{Rouse}, \\ n^{3\nu}F^{3(1-3\nu)/2} = m^{3\nu}F^{3(1-\nu)/2}, & \text{Zimm}. \end{cases} \tag{18}$$

The slopes in Fig. 8 on average are reading as 1.75 for athermal systems and 1.49 for theta systems, in good agreement with the theoretical values according to Zimm (1.764 and 1.5, respectively). Results obtained from the F dependence at constant n or constant m (see Table IV) are less convincing but still reasonable.

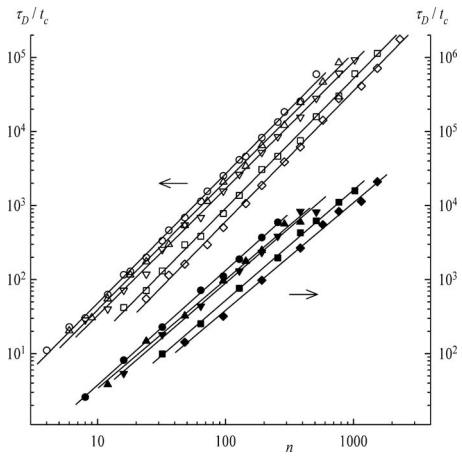

FIG. 8. Log-log plots of the translational diffusion time vs total number of bonds n for $a_{PS}=25$ (open symbols) and $a_{PS}=27.25$ (full symbols). Types of symbols are as in Fig. 1.

TABLE IV. Scaling exponents of the translational diffusion time obtained by DPD and predicted by the Daoud and Cotton model assuming Rouse or Zimm behavior.

	Athermal conditions			Theta conditions		
	F=const	n=const	m=const	F=const	n=const	m=const
DPD	1.75	−0.84	0.96	1.49	−0.70	0.80
Rouse	2.176	−0.764	1.412	2	−0.5	1.5
Zimm	1.764	−1.146	0.618	1.5	−0.75	0.75

IV. CONCLUSIONS

Since global properties of dynamic nature evolve very slowly in polymeric systems, large time scales have to be covered by computer simulations in order to gain realistic values for, e.g., the diffusion coefficient in a direct fashion by analyzing the msd. At present, this goal can be reached by coarse-grained techniques using larger time steps and less particles by treating several single molecules as one "bead". Due to the fact that modes of motion contributing to overall displacement occur at different but not well separated time scales, the degree of coarse graining has to be chosen in a way that still ensures a correct treatment of hydrodynamics. It has been shown in the present paper that a method well adapted to these demands is DPD. In this mesoscopic MD technique, a polymer chain is treated as a freely jointed equivalent chain consisting of several purely repulsive beads, linked together by springs. Various types of polymers including star-branched chains (investigated here) can be easily implemented in this way. Such a chain evolves in a bath of single beads, which act as a solvent. Their explicit treatment and the preservation of Galilean invariance give rise to momentum transport within the fluid and thus allow for correct hydrodynamic interaction. In addition, static properties such as size and shape of the solute are accessible as well and in full accordance with results of other simulation techniques. Furthermore, at least in principle, a transformation of experimentally obtained Flory–Huggins parameters characteristic for specific polymers into simulation parameters should be possible,[42] as well as the backtransformation of the simulation results into the atomistic picture. This latter point, however, is deferred to further investigations.

ACKNOWLEDGMENTS

We are grateful for funding from the Austrian Science Fund FWF (Grant No. P20124). Parts of these calculations were performed on the Schrödinger Linux Cluster of the University of Vienna which is gratefully acknowledged.

[1] *Monte Carlo and Molecular Dynamics Simulations in Polymer Science*, edited by K. Binder (Oxford University Press, New York, 1995).
[2] D. Frenkel and B. Smit, *Understanding Molecular Simulation*, Computational Science Series (Academic, San Diego, 2002).
[3] *Bridging Time Scales: Molecular Simulations for the Next Decade*, Lecture Notes in Physics Vol. 605, edited by P. Nielaba, M. Mareschal, and G. Ciccotti (Springer, Berlin, 2002).
[4] *Simulation Methods for Polymers*, edited by M. Kotelyanskii and D. N. Theodorou (Marcel Dekker, New York, 2004).
[5] V. Galiatsatos, *Molecular Simulation Methods for Predicting Polymer Properties* (Wiley, New York, 2005).

[6] A. R. Leach, *Molecular Modelling* (Pearson, Essex, 2001).
[7] G. Zifferer and A. Kornherr, J. Chem. Phys. **122**, 204906 (2005).
[8] D. N. Theodorou, in *Bridging Time Scales: Molecular Simulations for the Next Decade*, Lecture Notes in Physics Vol. 605, edited by P. Nielaba, M. Mareschal, and G. Ciccotti (Springer, Berlin, 2002), Chap. 3.
[9] G. Zifferer, T. Petrik, B. Neubauer, and O. F. Olaj, Macromol. Symp. **181**, 331 (2002) and references cited therein.
[10] A. Kolinski and A. Sikorski, J. Polym. Sci., Polym. Chem. Ed. **20**, 3147 (1982); A. Sikorski, A. Kolinski, *ibid.* **22**, 97 (1984).
[11] G. Zifferer, Macromol. Theory Simul. **8**, 433 (1999).
[12] A. Sikorski, Macromol. Theory Simul. **9**, 564 (2000).
[13] A. Sikorski, Macromolecules **35**, 7132 (2002).
[14] G. Xu and W. L. Mattice, Macromol. Theory Simul. **11**, 649 (2002).
[15] H.-P. Hsu, W. Nadler, and P. Grassberger, Macromolecules **37**, 4658 (2004).
[16] C. H. Vlahos, A. Horta, N. Hadjichristidis, and J. J. Freire, Macromolecules **28**, 1500 (1995).
[17] C. Vlahos, Y. Tselikas, N. Hadjichristidis, J. Roovers, A. Rey, and J. J. Freire, Macromolecules **29**, 5599 (1996).
[18] P. H. Nelson, G. C. Rutledge, and T. A. Hatton, Comput. Theor. Polym. Sci. **8**, 31 (1998).
[19] A. M. Rubio, P. Brea, J. J. Freire, and C. Vlahos, Macromolecules **33**, 207 (2000).
[20] R. Connolly, E. G. Timoshenko, and Y. A. Kuznetsov, J. Chem. Phys. **119**, 8736 (2003).
[21] J. Havrankova, Z. Limpouchova, and K. Prochazka, Macromol. Theory Simul. **12**, 512 (2003).
[22] Y. Chang, W.-C. Chen, Y.-J. Sheng, S. Jiang, and H.-K. Tsao, Macromolecules **38**, 6201 (2005).
[23] J. J. Freire, Adv. Polym. Sci. **143**, 35 (1999).
[24] G. S. Grest, L. J. Fetters, J. S. Huang, and D. Richter, in *Polymeric Systems*, Advanced Chemical Physics Vol. XCIV, edited by I. Prigogine and S. A. Rice (Wiley, New York, 1996), Chap. 2.
[25] S.-J. Su and J. Kovac, J. Phys. Chem. **96**, 3931 (1992).
[26] T. Pakula, S. Geyler, T. Edling, and D. Boese, Rheol. Acta **35**, 631 (1996).
[27] T. Pakula, D. Vlassopoulos, G. Fytas, and J. Roovers, Macromolecules **31**, 8931 (1998).
[28] L. A. Molina and J. J. Freire, Macromolecules **32**, 499 (1999).
[29] J. J. Freire, L. A. Molina, A. Rey, and K. Adachi, Macromol. Theory Simul. **8**, 321 (1999).
[30] C. von Ferber, A. Jusufi, M. Watzlawek, C. N. Likos, and H. Löwen, Phys. Rev. E **62**, 6949 (2000).
[31] D. Vlassopoulos, G. Fytas, T. Pakula, and J. Roovers, J. Phys.: Condens. Matter **13**, R855 (2001).
[32] A. Di Cecca and J. J. Freire, Macromolecules **35**, 2851 (2002).
[33] A. Di Cecca and J. J. Freire, Polymer **44**, 2589 (2003).
[34] I. Carmesin and K. Kremer, Macromolecules **21**, 2819 (1988).
[35] H. P. Deutsch and K. Binder, J. Chem. Phys. **94**, 2294 (1991).
[36] M. Watzlawek, C. N. Likos, and H. Löwen, Phys. Rev. Lett. **82**, 5289 (1999).
[37] H.-P. Hsu and P. Grassberger, Europhys. Lett. **66**, 874 (2004).
[38] A. Malevanets and R. Kapral, J. Chem. Phys. **110**, 8605 (1999).
[39] K. Mussawisade, M. Ripoll, R. G. Winkler, and G. Gompper, J. Chem. Phys. **123**, 144905 (2005).
[40] M. Ripoll, R. G. Winkler, and G. Gompper, Phys. Rev. Lett. **96**, 188302 (2006).
[41] P. J. Hoogerbrugge and J. M. V. A. Koelman, Europhys. Lett. **19**, 155 (1992).
[42] R. D. Groot and P. B. Warren, J. Chem. Phys. **107**, 4423 (1997).
[43] H.-J. Qian, L.-J. Chen, Z.-Y. Lu, Z.-S. Li, and C.-C. Sun, J. Chem. Phys. **124**, 014903 (2006).
[44] R. E. van Vliet, H. C. J. Hoefsloot, and P. D. Iedema, Polymer **44**, 1757 (2003).
[45] J. Xia and C. Zhong, Macromol. Rapid Commun. **27**, 1110 (2006).
[46] S.-H. Chou, H.-K. Tsao, and Y.-J. Sheng, J. Chem. Phys. **125**, 194903 (2006).
[47] Y.-J. Sheng, C.-H. Nung, and H.-K. Tsao, J. Phys. Chem. B **110**, 21643 (2006).
[48] P. Español, Phys. Rev. E **52**, 1734 (1995).
[49] C. Pierleoni and J. Ryckaert, J. Chem. Phys. **96**, 8539 (1992).
[50] G. Zifferer, Macromol. Theory Simul. **9**, 479 (2000).
[51] H. Müller-Krumbhaar and K. Binder, J. Stat. Phys. **8**, 1 (1973); G. Zifferer, Macromolecules **23**, 3166 (1990) and references cited therein.
[52] J. des Cloizeaux and G. Jannink, *Polymers in Solution* (Clarendon, Oxford, 1990).
[53] A. G. Schlijper, P. J. Hoogerbrugge, and C. W. Manke, J. Rheol. **39**, 567 (1995).
[54] Y. Kong, C. W. Manke, W. G. Madden, and A. G. Schlijper, J. Chem. Phys. **107**, 592 (1997).
[55] V. Symeonidis, G. E. Karniadakis, and B. Caswell, Phys. Rev. Lett. **95**, 076001 (2005).
[56] N. A. Spenley, Europhys. Lett. **49**, 534 (2000).
[57] J. M. Ilnytskyi and Y. Holovatch, Condens. Matter Phys. **10**, 539 (2007).
[58] W. Jiang, J. Huang, Y. Wang, and M. Laradji, J. Chem. Phys. **126**, 044901 (2007).
[59] B. Dünweg, D. Reith, M. Steinhauser, and K. Kremer, J. Chem. Phys. **117**, 914 (2002).
[60] M. Daoud and J. P. Cotton, J. Phys. (Paris) **43**, 531 (1982).
[61] T. M. Birshtein and E. B. Zhulina, Polymer **25**, 1453 (1984).
[62] G. S. Grest, K. Kremer, and T. A. Witten, Macromolecules **20**, 1376 (1987).
[63] B. H. Zimm and W. H. Stockmayer, J. Chem. Phys. **17**, 1301 (1949).
[64] G. S. Grest and M. Murat, in *Monte Carlo and Molecular Dynamics Simulations in Polymer Science*, edited by K. Binder (Oxford University Press, New York, 1995), Chap. 9.
[65] J. J. Freire, J. Pla, A. Rey, and R. Prats, Macromolecules **19**, 452 (1986); J. J. Freire, A. Rey, and J. G. de la Torre, *ibid.* **19**, 457 (1986).
[66] J. Batoulis and K. Kremer, Europhys. Lett. **7**, 683 (1988).
[67] A. Rey, J. J. Freire, M. Bishop, and J. H. R. Clarke, Macromolecules **25**, 1311 (1992).
[68] K. Šolc and W. H. Stockmayer, J. Chem. Phys. **54**, 2756 (1971).
[69] K. Šolc, J. Chem. Phys. **55**, 335 (1971).
[70] J. Mazur, Ch. M. Guttman, and F. L. McCrackin, Macromolecules **6**, 872 (1973); M. Bishop and J. P. J. Michels, J. Chem. Phys. **85**, 5961 (1986); M. Bishop and C. J. Saltiel, *ibid.* **88**, 6594 (1988); H. W. Diehl and E. Eisenriegler, J. Phys. A **22**, L87 (1989); O. Jagodzinski, E. Eisenriegler, and K. Kremer, J. Phys. I **2**, 2243 (1992); G. Wei, Macromolecules **30**, 2130 (1997).
[71] P. E. Rouse, Jr., J. Chem. Phys. **21**, 1272 (1953).
[72] B. H. Zimm, J. Chem. Phys. **24**, 269 (1956).
[73] J. G. Kirkwood and J. Riseman, J. Chem. Phys. **16**, 565 (1948).
[74] M. P. Allen and D. J. Tildesley, *Computer Simulation of Liquids* (Oxford Science, Oxford/Clarendon, New York, 1993).
[75] B. Dünweg and K. Kremer, J. Chem. Phys. **99**, 6983 (1993).